Delignified and densified cellulose materials with superior mechanical properties for sustainable engineering

Marion Frey[12], Daniel Widner[12], Jana Segmehl[12], Kirstin Casdorff[12], Tobias Keplinger[12], Ingo Burgert[12]*

[1] Wood Materials Science, Institute for Building Materials, ETH Zürich, Stefano-Franscini Platz 3, 8093 Zürich, Switzerland

[2] Bio-inspired Wood Materials, Applied Wood Materials, EMPA, Überlandstrasse 129, 8600 Dübendorf, Switzerland

KEYWORDS:Cellulose scaffolds, shear-assisted densification, natural fiber reinforced composites, delignification, wood modification, AFM

ABSTRACT

Today`s materials research aims at superior mechanical performance in combination with advanced functionality. In this regard great progress has been made in tailoring materials by assembly processes in bottom-up approaches. In the field of wood-derived materials, nanocellulose research has gained increasing attention and materials with advanced properties were developed. However, there are still unresolved issues concerning upscaling for large scale applications. Alternatively, the sophisticated hierarchical scaffold of wood can be utilized in a top-down approach to upscale functionalization and one can profit at the same time from its renewable nature, CO_2 storing capacity, light weight and good mechanical performance. Nevertheless, for

bulk wood materials a wider multi-purpose industrial use is so far impeded by concerns regarding durability, natural heterogeneity as well as limitations in terms of functionalization, processing and shaping. Here we present a novel cellulose material concept, based on delignification and densification of wood resulting in a high performance material. A delignification process using hydrogen peroxide and acetic acid was optimized to delignify entire wooden blocks and to retain the highly beneficial structural directionality of wood. In a subsequent step, these cellulosic blocks were densified in a process combining compression and lateral shear in order to gain a very compact cellulosic material with entangled fibres while retaining unidirectional fibre orientation. The cellulose materials obtained by different densification protocols were structurally, chemically and mechanically characterized revealing superior mechanical performance compared to native wood. Furthermore, after delignification the cellulose material can be easily formed into different shapes and the delignification facilitates functionalization of the bio-scaffold.

INTRODUCTION

In producing wood, trees provide an excellent renewable biomaterial comprising high specific strength and stiffness.[1] The hierarchical structure and fibrous architecture with aligned fibers, which are composed of rigid cell walls that consist of high-strength cellulose fibrils embedded in a pliant matrix of hemicelluloses and lignin, has been a great source of inspiration for the design of engineered composites.[2] In recent years, there has been an increasing number of publications that report on the functionalization of the sophisticated wood structure to develop materials with novel properties,[3] including transparency,[4] magnetism[5], electrical properties,[6] stimuli-responsiveness[7] as well as for filtration and oil-water separation purposes.[8] These are so far mainly fundamental works that show the principle approach and the application potential, but for a broader

utilization and implementation of such wood materials in high-end applications certain limitations need to be overcome. These mainly arise from the heterogeneity of the wood substrate, causing a low reliability in terms of material properties and little control of the efficacy of the functionalization.

Since wood is the product of a natural growth process influenced by environmental factors, its tissue structure, and hence density can vary substantially within a species and even within a trunk of an individual tree. Furthermore, mechanical adaptations during the life of the tree at the tissue and fiber level or the presence of natural features such as knots result in additional variability, which leads to concerns regarding the reliability of wood, respectively predictability in high-performance applications. A prominent process to achieve a higher homogeneity of wood and to preserve the structural directionality is densification, since the density is one of the dominating factors dictating mechanical properties.[9] Wood samples can be compressed to reach high and homogenous density levels accompanied by significant mechanical property improvements.[10] Partial delignification of wood facilitates densification processes and infiltration with resins can result in strong natural fibre-reinforced composites.[11]

Moreover, it is difficult to functionalize the compact wood cell wall. Thus only a very limited number of bulk wood modifications have been successfully commercialized,[12] while with many other approaches, property improvements could only be achieved by rather complex chemistries.[13] Hence, in the last two decades a strong focus has been laid on the decomposition of wood down to the nanoscale, enabling the use of delignified cellulosic material including nanofibrillated cellulose and cellulose nanocrystals. The utilization of this type of cellulose materials further allows for the application of simple and versatile functionalization approaches.[14 14c, 15] However, so far it is a great challenge to transfer the mechanical performance of the individual units to the bulk

composite material as fibre re-orientation and assembly are difficult to achieve. Although great progress was made towards nanocellulose re-orientation in micro-fluidic devices[16] and in 3D- or even 4D-printing processes,[17] it remains a challenge to achieve nanocellulose-based materials with excellent mechanical performance at the macroscale.

Here we present a novel cellulose material, which was obtained by a subsequent combination of delignification and densification while retaining the beneficial hierarchical structure and fiber directionality of wood.[18] The obtained cellulose material was structurally, chemically and mechanically characterized at different length scales as illustrated in Figure 1. For mechanical analysis at the macroscopic level tensile tests were conducted and the influence of densification on the folding behavior of earlywood cells was examined by light microscopy and SEM at the tissue level. Structural changes at the cell wall level due to delignification and densification were studied on latewood cells by AFM measurements.

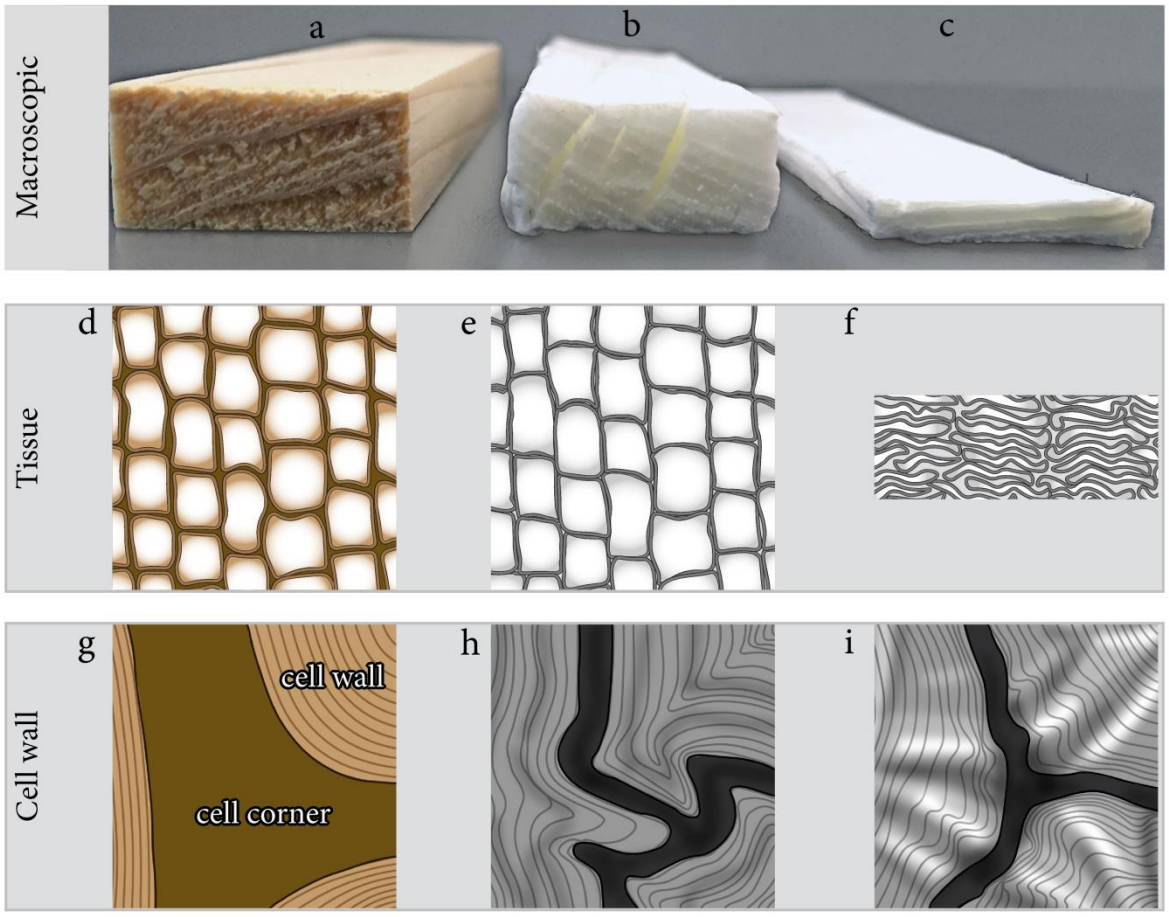

Figure 1. Delignification of native wood **(a, d, g)** results in a white cellulose scaffold **(b, e)**. The matrix lignin is removed between the cells **(e)** and in the cell wall, which results in a flexible cell wall **(h)**. Densification of the delignified cellulose scaffold **(c)** results in a homogenous folding of the earlywood cells **(f)** and in wrinkling of latewood cells **(i)**.

EXPERIMENTAL SECTION

Delignification procedure. Norway spruce samples were cut to the dimensions 100 x 10 x 20 mm^3 (longitudinal x radial x tangential). Eight samples per variant were cut from the same height in the

trunk from matched positions in order to obtain similar growth ring patterns. The pieces were stored at 20 °C/65 % rel. humidity before treatment. Afterwards, the wood samples were placed into a beaker on top of a metal-grid sample holder. An equal-volume mixture of hydrogen peroxide solution (35 wt-%, Acros Organics) and glacial acetic acid (Fisher Chemicals) was prepared. The wood pieces were infiltrated over night at room temperature under stirring. The solution was then heated and the pieces were delignified for 6 h at 80 °C. Infiltration (overnight) and delignification (6 h, 80 °C) processes were repeated once with a fresh H_2O_2-HAc solution.[19] After delignification, the samples were washed in water with an exchange of the water for five times daily until the pH value of the water was above 4.5. To retain the structural integrity of the samples, they were confined in a metal-grid clamp during the washing step. After washing, samples were conditioned until a constant mass was obtained.

*Weight loss, volume loss, density***.** Mass and volume of the samples were measured before and after the delignification step and after densification. Measurements were conducted after conditioning the samples at 65% relative humidity. Comparing mass and volume of native wood to the values obtained for the delignified cellulose scaffolds allowed for calculating the weight and volume loss and the change in density caused by the delignification.

Fourier transform infrared (FTIR) spectroscopy. Thin slices of delignified wood pieces were analyzed with a FT-IR spectrometer (Bruker Tensor 27). Spectra were baseline corrected (concave rubberband) and normalized (min/max) in the OPUS software and plotted in Origin 2016.

Densification procedure. Delignified wood pieces were densified in radial direction using a universal testing machine (Zwick Roell, 100 kN load cell) in compression mode.[18] A punch was pressed stepwise (1 mm compression, 15 s waiting time) into the mold containing the specimen

(100 x 20 mm^2). Prior to densification the delignified wood pieces were either conditioned at 20°C and 65% relative humidity or at 20°C and 95% relative humidity. During the densification process the specimens were compressed from an initial thickness of 10 mm to a final thickness of 3.5 mm for low force (LF) densification and of 2.5 mm for high force (HF) densification (see Figure S1 for the force and displacement regime of the latter). For both moisture contents and force conditions an additional lateral movement of the punch was applied during compression. This lateral movement was induced by an air compressor gun (2 bar) connected to the punch. After densification, the densified pieces were conditioned at 20 °C/65 % relative humidity. For each variant, seven samples were used for tensile testing and the remaining sample was used for characterization by light microscopy and SEM. As an additional reference, native wood was densified resulting in a thickness of the specimens of approximately 5.5 mm.

Tensile testing. The outer parts of the edges were cut and the specimens were grinded (sandpaper grit size 200 & 600) to achieve regular cross-sections prior to testing of the tensile properties of the specimens in a Zwick Roell (100 kN load cell). The distance between the clamps was determined with 36 mm and the displacement was measured with a video extensometer, detecting two indicator strips placed on the specimen surface with an initial distance of 25 mm. The tests were conducted at 20°C and 65% relative humidity at a speed of 5 mm/min until a 30 % force drop after the maximal force (Fmax) had been reached. The tensile strength and the tensile modulus were calculated based on Fmax and on the slope between 10 % - 30 % of Fmax, respectively. The work until fracture was calculated as the integral of the force-distance curve until failure of the sample.

Microtome & Ultramicrotome Cutting. The samples surfaces characterized by light microscopy (Olympus BX51) and AFM (JPK Instruments AG) were prepared using a rotary microtome (Leica

Ultracut, Germany). Samples for AFM measurements were additionally cut using an ultramicrotome (Reichert Jung-Ultracut) with a diamond knife (Diatome).

Atomic force microscopy (AFM). AFM imaging was performed using a NanoWizard 4 (JPK Instruments AG) in the Quantitative Imaging mode (QI) at 20 °C and 65% relative humidity.[20] The resolution was set to 256 x 256 pixels and the scan size was 20 x 20 µm. A non-contact cantilever (NCHR, NanoWorld, resonance frequency 320 kHz) with a silicon probe was used. The setpoint was set to 60 nN, the z-length to 100 nm and the pixel time was set to 12 ms. Calibration of the cantilever was done with the thermal noise method. The generated images were processed with the JPK image processing software (JPK Instruments AG).

Scanning electron microscopy (SEM). Delignified and densified wood pieces were coated with a sputter coater (CCU-010, Safematic, Switzerland). A Pt-Pd (80/20) coating of ~6 nm thickness was applied. For the measurements a Hitachi SU5000 was used.

RESULTS AND DISCUSSION

In a first step, spruce wood was delignified with an equal-volume mixture of hydrogen peroxide and acetic acid,[19] removing all lignin and parts of the hemicelluloses as can be seen in terms of changes of respective peaks in the IR spectra (Figure 2).

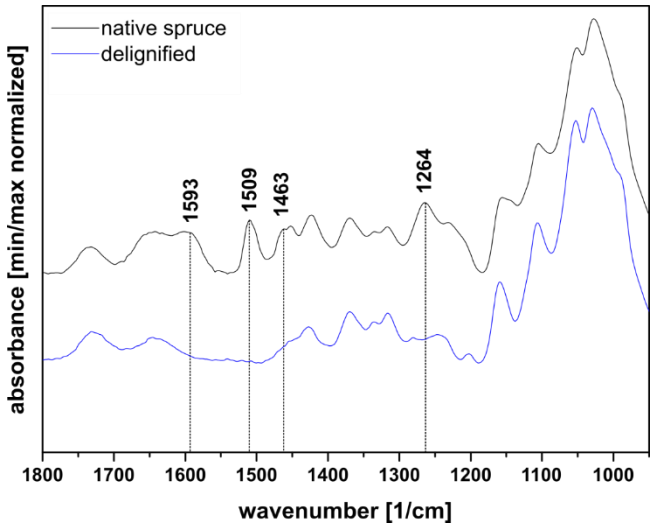

Figure 2. FTIR spectra of native and delignified spruce wood samples in the spectral range from 1800 to 900 cm^{-1}. The absence of characteristic lignin peaks at 1593 cm^{-1}, 1460 cm^{-1}, 1509 cm^{-1} (aromatic skeletal vibration) and 1264 cm^{-1} (guaiacyl ring breathing with CO stretching)[1] confirm a complete removal of lignin. Changes in the area from 1200 to 1000 cm^{-1} mainly arise from the reduction of hemicelluloses.

The complete lignin removal can be directly concluded from the entire absence of the lignin specific IR bands, whereas changes in hemicelluloses are obvious in the spectral range from 1000 1/cm – 1200 1/cm, but a detailed quantification of the content is limited because of the partial overlap with cellulose bands. However, the loss of hemicelluloses can be estimated by taking the total mass loss of 40% during delignification into account (Fig S2). According to literature values, spruce wood consists of ~31% hemicelluloses and ~28% lignin,[21] which results in a reduction of hemicellulose content of around one-third. Moreover, the densification process does not only result in a mass reduction but also in a volume loss of more than 20% (Figure 3b, and S2). It can be assumed that this leads in total to a higher porosity of the specimens, as the

entire density is reduced from 440 kg/m³ in the native state to 330 kg/m³ in the delignified state, respectively.

In a subsequent step, the cellulose material was densified to a defined thickness, while simultaneously applying lateral shear.[18] Two different densification levels termed low force densification and high force densification were applied and distinguished on the basis of the targeted and achieved sample height after the densification. Furthermore, the densification was conducted at two different equilibrium moisture contents adjusted at 65% relative humidity and 95 % relative humidity, respectively. Figure 3 shows the forces that were applied to achieve the targeted specimen heights and the resulting densities in all tested sample categories.

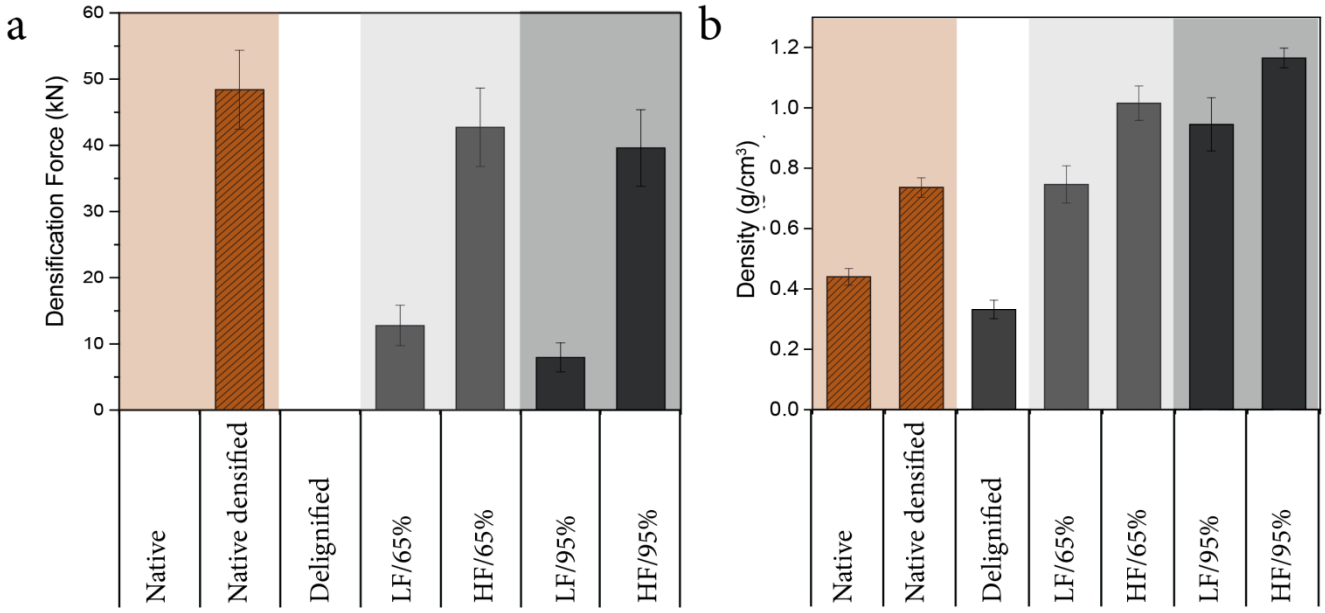

Figure 3. Densification force **(a)** and resulting densities **(b)** of all sample categories. Higher humidity in the delignified scaffold results in lower densification forces and higher densities.

The delignification process facilitates cell collapse during densification,[11b] most probably due to a reduction of the transverse rigidity of the cell walls. Delignified cells were smoothly compressed and almost no cracks could be observed in the cell walls, whereas densified native (lignified) wood showed extensive cell wall cracking, in particular in the latewood region (Fig. S3). After delignification and low force densification a cell folding of the thin-walled earlywood cells could be observed (Fig. 4). Highly compressed latewood regions were only found after high force densification.

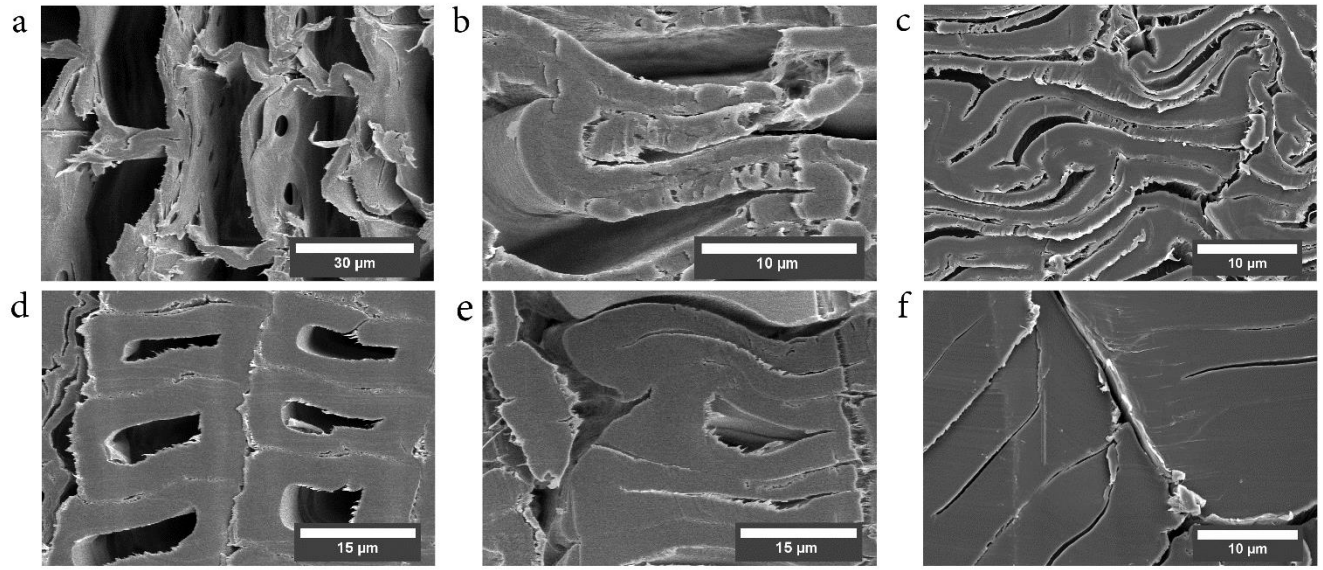

Figure 4. SEM images of earlywood **(a,b,c)** and latewood **(d,e,f)** cell walls before densification **(a,d)** and after low force densification **(b,e)** and high force densification **(c,f)** with applying lateral shear.

The combination of compressive and lateral shear forces affected the structural organization of the cellulose material at two hierarchical levels. Light microscopy images showing the cell and

tissue level, reveal in agreement with the SEM investigations, that a densification at low-force after equilibration at 65 % relative humidity, resulted in a collapse of the earlywood cells, but that the more compact latewood cells were not fully compressed. A zoom in the earlywood zone reveals a very regular transverse folding of cells at the tissue level (Figure 5b), whereas for specimens that were densified without applying lateral shear, a more irregular and uneven cell collapse was found (Figure 5e). Additionally, the shear affected the mode of cell wall deformation during the process. AFM studies showed that the thick cell walls of samples that were densified without lateral shear were more wrinkled and distorted while the samples that were densified with lateral shear possessed more smoothly compressed cell walls (Figure 5c,f).

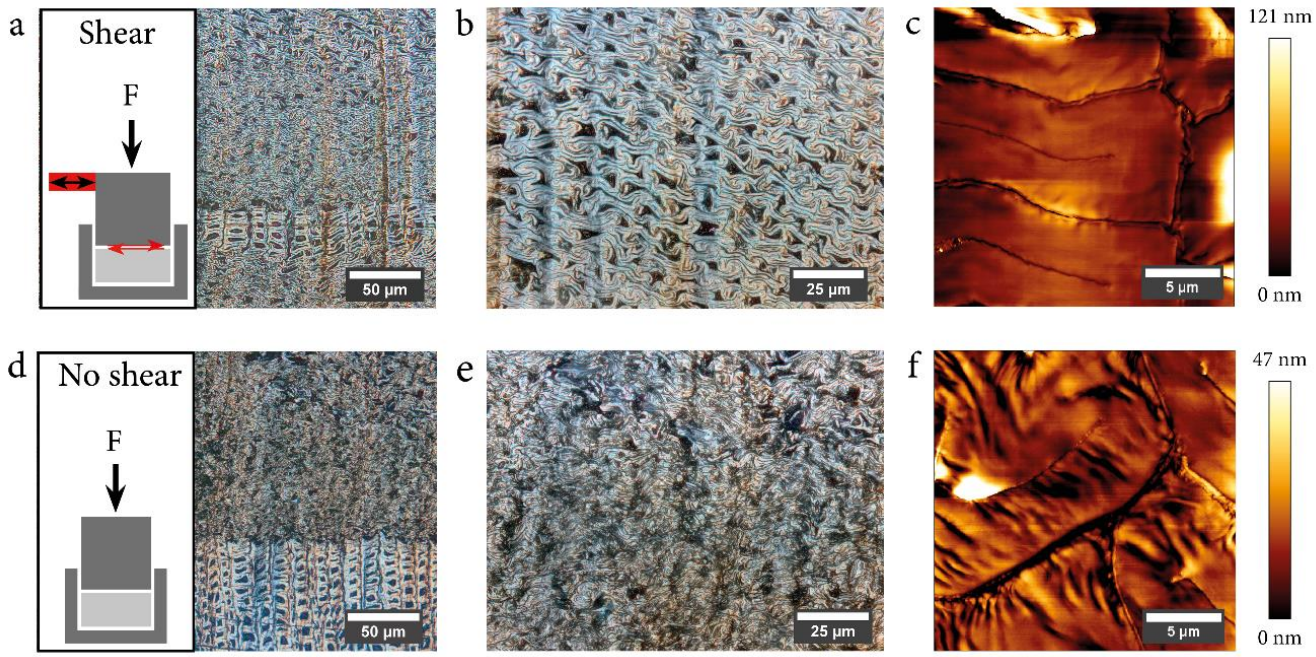

Figure 5. Delignified specimen densified at low-force after equilibration at 65 % relative humidity. A zoom into earlywood region by light microscopy **(b,e)** shows that folding of earlywood cells is more homogenous, when lateral shear is applied during densification. AFM images of densified

latewood cells with shear **(c)** and without shear **(f)** during densification reveal the smoothening effect of shearing on the cell wall level.

Tensile tests of the cellulose specimens show that remarkable material properties can be achieved. It is important to emphasize that the tested samples were totally resin-free and therefore only the bond forces between the aligned cells and cellulose fibrils were decisive. The different levels of densification and relative humidity affected the obtained mechanical properties (Figure 6).

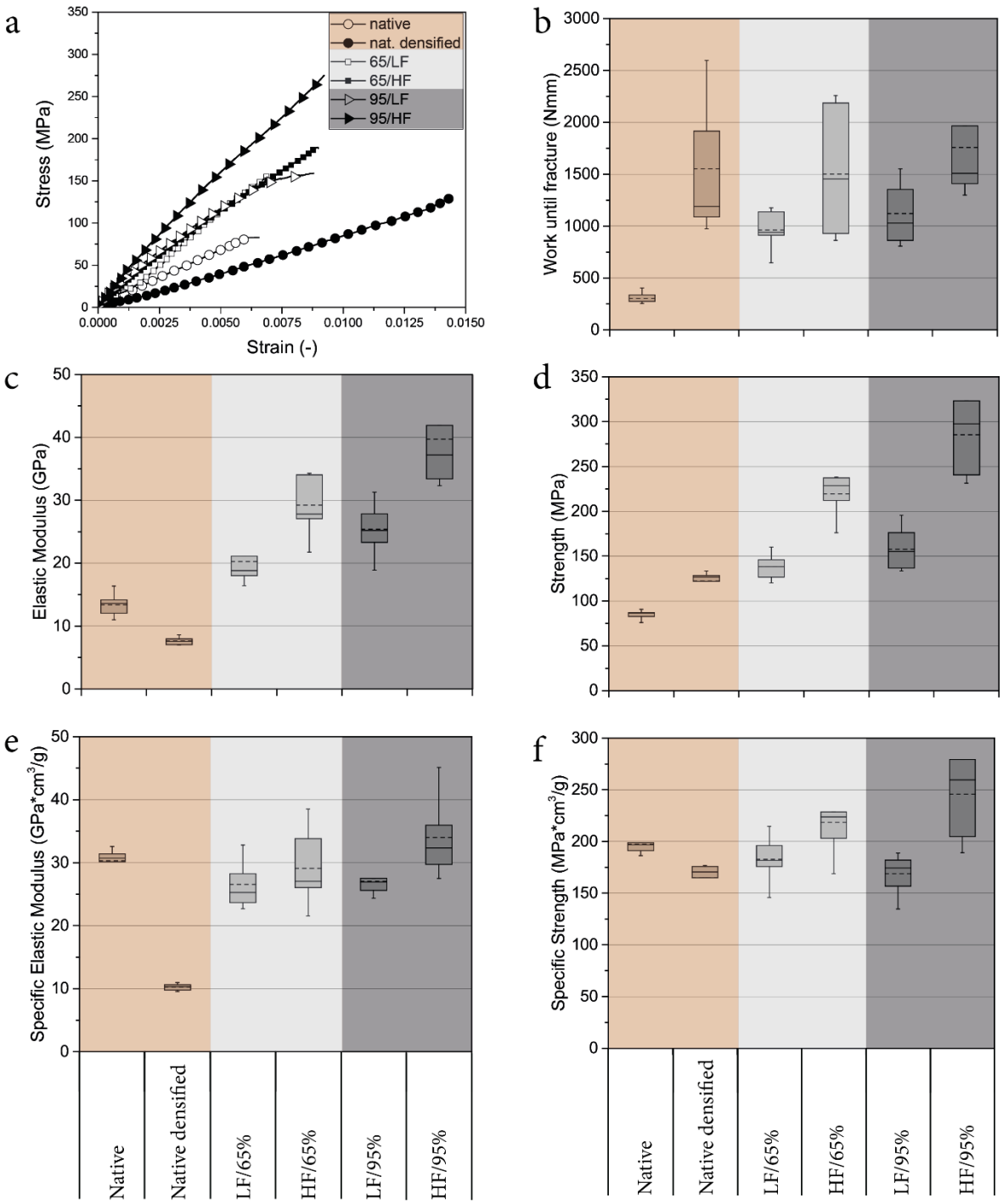

Figure 6. Mechanical characterisation of the reference samples (native, native densified) and of shear assisted densified cellulose scaffolds conditioned at 20°C and 65% relative humidity by longitudinal tensile tests. **a,** Representative stress-strain curves for each treatment. **b,** Work until

fracture (**b:** n=8 for native; n=5 for native densified, LF/65%, LF/95%; n=7 for HF/65%, n=6 for HF/95%). **c,** Elastic modulus. **d,** Strength. **e**, Specific elastic modulus. **f**, Specific strength (**c-f:** n=8 for native; n=6 for native densified; n=5 for LF/65%; n=7 for LF/95%, HF/65%, HF/95%).

The stress-strain curves of representative tests show the severe impact of the densification treatment on the mechanical behavior (Fig. 6a). A comparison of the elastic moduli of the samples indicated that compression with higher forces results in higher values and that higher humidity levels are favorable and hence superior properties are achieved by a strong densification of samples conditioned at high relative humidity (95% RH) (Figure 6c). A very similar trend was obtained for the tensile strength, again showing that strong densification is superior to light densification and that a compression at high humidity levels outperforms compression at low humidity levels (Figure 6d). Remarkably, in comparison to native spruce (Young`s modulus ~13 GPa, tensile strength ~80 MPa) an up to three times higher stiffness could be achieved and also the tensile strength was succeeded by a factor of three for the highly densified samples. Contrary the application of the same densification protocol to native spruce resulted in a loss in elastic modulus and a moderate increase in strength, underlining the crucial relevance of the delignification for the loss of transverse cell wall rigidity in this particular process. Eliminating the influence of density differences by calculating the specific elastic moduli and the specific tensile strengths (Fig 6e,f) shows that material improvements can particularly be achieved for specimens densified at high humidity and high compression forces.

Furthermore, the work until fracture of the cellulose materials was calculated on the basis of the tensile tests (Fig 6b). These calculations could only consider the mechanical response until a strain at which the two indicator strips on the specimen surface for displacement detection were misaligned due to fracture events. However, the obtained results indicate that the cellulose

materials compressed with high force reach higher values compared to the specimens compressed with low force. The densified native wood specimens reached work until fracture values similar to the delignified specimens compressed at high force, but their elastic modulus was much lower. This interrelation can be illustrated by comparing the sample categories on the basis of elastic moduli and work until fracture (Fig. 7)

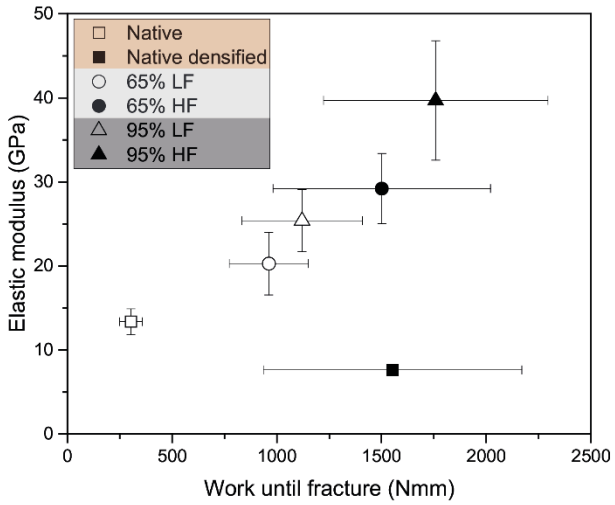

Figure 7. Comparison of elastic modulus and work until fracture of the different categories of cellulose material. All error bars represent the standard deviation (n=8 for native; n=5 for native densified, LF/65%, LF/95%; n=7 for HF/65%, n=6 for HF/95%).

The comparison in Figure 7 shows that the applied delignification and densification protocols allow for producing cellulose materials with a highly desired material property combination of improved stiffness and toughness. In particular the specimens that were densified with high force at high moisture content show superior properties for both mechanical parameters. This combination can be found in several biological systems (e.g. bone),[22] but a transfer to engineering materials is challenging.

Besides the improved mechanical performance, the material concept has the major advantage that the delignified samples can be easily deformed and elements with different shapes and complex geometries can be produced by non-cutting processes (Figure 8).

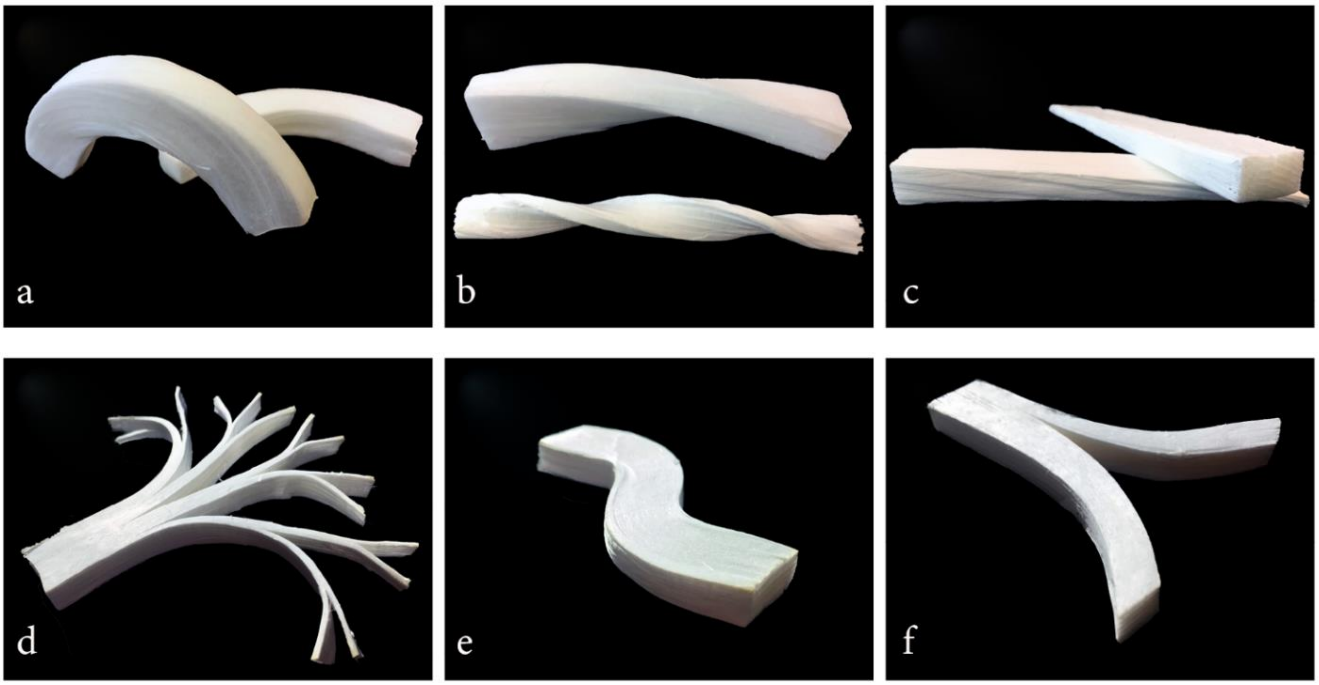

Figure 8. Elements of different shapes and geometries with perfectly aligned fibers. **a,e,** curved. **b,** twisted. **c,** graded. **d,f,** branched. The structures can be manufactured by simply forming the cellulose scaffold in wet state.

Remarkably, even for high curvatures the fibers are kept perfectly oriented related to the distribution of forces and no fibers need to be cut as known to be common in current wood processing techniques. This makes curved or twisted structures (Figure 8) more mechanically robust and vast applicable as load-bearing elements. Further, the material's flexibility also allows for easily designing connections that fully respect fiber alignment, as it is known for many biological role models, for instance in tree or cacti branching.[23] Connecting fibrous elements has

ever been a challenge in fiber composite design, as an interweaving of fibers is needed to sufficiently transfer forces between two connected elements. Moreover, the level of densification can be easily varied within individual elements, for the design of composites with gradual alterations in height, density and stiffness.

The here presented cellulose materials have been fabricated without the addition of an adhesive system. However, considering the effect of delignification, an eased insertion of thermoplastics or thermosets into the cellulose scaffolds can be expected. Such an insertion would most likely provide higher strength and toughness. Although the individual crystalline cellulose unit possesses a very high stiffness and strength[24] and also single plant fibers from hemp, flax or bamboo are known for exceptional tensile properties,[25] it remains a challenge to transfer these performances to the macroscopic composites. There are only a few examples, like bamboo-epoxy composites or wood polymer composites that have reached superior mechanical properties.[11, 26] Natural fibre composites that are based on embedding single fibres in a matrix have by far lower stiffnesses and strengths,[27] which clearly shows the advantage in retaining the natural fibre assembly for the production of bio-based engineering composites. Hence, the presented novel cellulose composites represent an important step forward towards high performance load bearing applications based on renewable lignocellulosic materials.

CONCLUSION.

A novel cellulose material was developed in a stepwise process of delignification and subsequent shear assisted densification, which resulted in a fibre folding and improved mechanical performance. Even without adding a matrix system the obtained mechanical properties were superior to wood and many other natural fibre-reinforced composites. For the strongly densified

95% RH samples an average elastic modulus of ~40 GPa and a tensile strength of ~300 MPa were reached. This is accompanied by a high work until fracture, which in combination with the high stiffness is highly desired. Furthermore, the composites can be easily pre-formed to different shapes and the delignification facilitates functionalization treatments. Based on the mechanical performances obtained and in view of their origin from a highly abundant and renewable resource, these sustainable cellulose materials are predestined for novel fibre-reinforced biocomposites.

ASSOCIATED CONTENT

Supporting Information

Mass and volume change as a result of the delignification procedure, densification curves (force-distance and tool distance-time), SEM images of densified native wood.

AUTHOR INFORMATION

Corresponding Author

*Ingo Burgert

E-mail: iburgert@ethz.ch

Author Contributions

MF: Performed experiments, analyzed data and co-wrote the manuscript; DW: Performed experiments and analyzed data; JS: Performed experiments and analyzed data; KC: Performed experiments and analyzed data; TK: Analyzed data and co-wrote the manuscript; IB: Designed the study, analyzed data and co-wrote the manuscript. All authors discussed the results and commented on the manuscript.

Notes

The authors declare no competing financial interest.

ACKNOWLEDGMENT. The authors would like to thank Thomas Schnider for technical support in the densification treatments and to the Scientific Center for Optical and Electron Microscopy (ScopeM) of ETH for providing the SEM and their technical support.

REFERENCES.

1. (a) Dunlop, J. W. C.; Fratzl, P., Biological Composites. *Annual Review of Materials Research, Vol 40* **2010,** *40*, 1-24; (b) Ashby, M. F.; F.R.S.; Easterling, K. E.; Harrysson, R.; Maiti, S. K., The fracture and toughness of woods. *Proc. R. Soc. Lond.* **1985,** *398*, 261-280.
2. (a) Jeronimidis, G., Design and function of structural biological materials. In *Structural biological materials - Design and structure-property relationships*, Elices, M., Ed. Pergamon: Amsterdam, 2000; pp 19-29; (b) Burgert, I., Materials Design Inspired by Tree and Wood Architecture. In *Materials Design Inspired by Nature: Function through Inner Architecture*, Fratzl, P.; Dunlop, J. W. C.; Weinkamer, R., Eds. Royal Soc Chemistry: Cambridge, 2013; pp 128-150.
3. (a) Burgert, I.; Cabane, E.; Zollfrank, C.; Berglund, L., Bio-inspired functional wood-based materials - hybrids and replicates. *International Materials Reviews* **2015,** *60* (8), 431-450; (b) Zhu, H. L.; Luo, W.; Ciesielski, P. N.; Fang, Z. Q.; Zhu, J. Y.; Henriksson, G.; Himmel, M. E.; Hu, L. B., Wood-Derived Materials for Green Electronics, Biological Devices, and Energy Applications. *Chem. Rev.* **2016,** *116* (16), 9305-9374.
4. (a) Li, Y. Y.; Fu, Q. L.; Yu, S.; Yan, M.; Berglund, L., Optically Transparent Wood from a Nanoporous Cellulosic Template: Combining Functional and Structural Performance. *Biomacromolecules* **2016,** *17* (4), 1358-1364; (b) Zhu, M. W.; Song, J. W.; Li, T.; Gong, A.; Wang, Y. B.; Dai, J. Q.; Yao, Y. G.; Luo, W.; Henderson, D.; Hu, L. B., Highly Anisotropic, Highly Transparent Wood Composites. *Adv. Mater.* **2016,** *28* (26), 5181-+.
5. (a) Merk, V.; Chanana, M.; Gierlinger, N.; Hirt, A. M.; Burgert, I., Hybrid Wood Materials with Magnetic Anisotropy Dictated by the Hierarchical Cell Structure. *Acs Applied Materials & Interfaces* **2014,** *6* (12), 9760-9767; (b) Trey, S.; Olsson, R. T.; Strom, V.; Berglund, L.; Johansson, M., Controlled deposition of magnetic particles within the 3-D template of wood: making use of the natural hierarchical structure of wood. *Rsc Advances* **2014,** *4* (67), 35678-35685.
6. (a) Chen, C. J.; Li, Y. J.; Song, J. W.; Yang, Z.; Kuang, Y.; Hitz, E.; Jia, C.; Gong, A.; Jiang, F.; Zhu, J. Y.; Yang, B.; Xie, J.; Hu, L. B., Highly Flexible and Efficient Solar Steam Generation Device. *Adv. Mater.* **2017,** *29* (30); (b) Chen, C. J.; Zhang, Y.; Li, Y. J.; Dai, J. Q.; Song, J. W.; Yao, Y. G.; Gong, Y. H.; Kierzewski, I.; Xie, J.; Hu, L. B., All-wood, low tortuosity, aqueous, biodegradable supercapacitors with ultra-high capacitance. *Energy Environ. Sci.* **2017,** *10* (2), 538-545; (c) Wan, J. Y.; Song, J. W.; Yang, Z.; Kirsch, D.; Jia, C.; Xu, R.; Dai, J. Q.; Zhu, M. W.; Xu, L. S.; Chen, C. J.; Wang, Y. B.; Wang, Y. L.; Hitz, E.; Lacey, S. D.; Li, Y. F.; Yang, B.; Hu, L. B., Highly Anisotropic Conductors. *Adv. Mater.* **2017,** *29* (41).
7. Keplinger, T.; Cabane, E.; Berg, J. K.; Segmehl, J. S.; Bock, P.; Burgert, I., Smart Hierarchical Bio-Based Materials by Formation of Stimuli-Responsive Hydrogels inside the Microporous Structure of Wood. *Advanced Materials Interfaces* **2016,** *3* (16).
8. (a) Chen, F. J.; Gong, A. S.; Zhu, M. W.; Chen, G.; Lacey, S. D.; Jiang, F.; Li, Y. F.; Wang, Y. B.; Dai, J. Q.; Yao, Y. G.; Song, J. W.; Liu, B. Y.; Fu, K.; Das, S.; Hu, L. B., Mesoporous, Three-Dimensional Wood Membrane Decorated with Nanoparticles for Highly Efficient Water Treatment. *Acs Nano* **2017,** *11* (4), 4275-4282; (b) Vidiella del Blanco, M.; Fischer, E. J.; Cabane, E., Underwater Superoleophobic Wood Cross Sections for Efficient Oil/Water Separation. *Advanced Materials Interfaces* **2017**.
9. Niemz, P.; Sonderegger, W., *Holzphysik*. Carl Hanser Verlag: Leipzig, 2017; p 580.

10. Navi, P.; Heger, F., Combined densification and thermo-hydro-mechanical processing of wood. *Mrs Bull* **2004,** *29* (5), 332-336.
11. (a) Shams, M. I.; Yano, H., A NEW METHOD FOR OBTAINING HIGH STRENGTH PHENOL FORMALDEHYDE RESIN-IMPREGNATED WOOD COMPOSITES AT LOW PRESSING PRESSURE. *Journal of Tropical Forest Science* **2009,** *21* (2), 175-180; (b) Shams, M. I.; Yano, H.; Endou, K., Compressive deformation of wood impregnated with low molecular weight phenol formaldehyde (PF) resin III: effects of sodium chlorite treatment. *Journal of Wood Science* **2005,** *51* (3), 234-238.
12. (a) Hill, C. A. S., *Wood Modification: Chemical, Thermal and Other processes*. John Wiley & Sons, Ltd: West Sussex, 2006; (b) Militz, H., The Improvement of Dimensional Stability and Durability of Wood through Treatment with Noncatalyzed Acetic-Acid Anhydrid. *Holz Als Roh-Und Werkstoff* **1991,** *49* (4), 147-152.
13. Cabane, E.; Keplinger, T.; Merk, V.; Hass, P.; Burgert, I., Renewable and Functional Wood Materials by Grafting Polymerization Within Cell Walls. *ChemSusChem* **2014,** *7* (4), 1020-1025.
14. (a) Laaksonen, P.; Walther, A.; Malho, J. M.; Kainlauri, M.; Ikkala, O.; Linder, M. B., Genetic Engineering of Biomimetic Nanocomposites: Diblock Proteins, Graphene, and Nanofibrillated Cellulose. *Angewandte Chemie-International Edition* **2011,** *50* (37), 8688-8691; (b) Zhang, Z.; Sebe, G.; Rentsch, D.; Zimmermann, T.; Tingaut, P., Ultralightweight and Flexible Silylated Nanocellulose Sponges for the Selective Removal of Oil from Water. *Chemistry of Materials* **2014,** *26* (8), 2659-2668; (c) Olsson, R. T.; Samir, M.; Salazar-Alvarez, G.; Belova, L.; Strom, V.; Berglund, L. A.; Ikkala, O.; Nogues, J.; Gedde, U. W., Making Flexible Magnetic Aerogels and Stiff Magnetic Nanopaper Using Cellulose Nanofibrils as Templates. *Nature Nanotechnology* **2010,** *5* (8), 584-588; (d) Gebauer, D.; Oliynyk, V.; Salajkova, M.; Sort, J.; Zhou, Q.; Bergstrom, L.; Salazar-Alvarez, G., A transparent hybrid of nanocrystalline cellulose and amorphous calcium carbonate nanoparticles. *Nanoscale* **2011,** *3* (9), 3563-3566.
15. (a) Henriksson, M.; Berglund, L. A.; Isaksson, P.; Lindstrom, T.; Nishino, T., Cellulose nanopaper structures of high toughness. *Biomacromolecules* **2008,** *9* (6), 1579-1585; (b) Tingaut, P.; Zimmermann, T.; Sebe, G., Cellulose nanocrystals and microfibrillated cellulose as building blocks for the design of hierarchical functional materials. *J. Mater. Chem.* **2012,** *22* (38), 20105-20111.
16. Hakansson, K. M. O.; Lundell, F.; Prahl-Wittberg, L.; Soderberg, L. D., Nanofibril Alignment in Flow Focusing: Measurements and Calculations. *Journal of Physical Chemistry B* **2016,** *120* (27), 6674-6686.
17. (a) Gladman, A. S.; Matsumoto, E. A.; Nuzzo, R. G.; Mahadevan, L.; Lewis, J. A., Biomimetic 4D printing. *Nat. Mater.* **2016,** *15* (4), 413-+; (b) Siqueira, G.; Kokkinis, D.; Libanori, R.; Hausmann, M. K.; Gladman, A. S.; Neels, A.; Tingaut, P.; Zimmermann, T.; Lewis, J. A.; Studart, A. R., Cellulose Nanocrystal Inks for 3D Printing of Textured Cellular Architectures. *Advanced Functional Materials* **2017,** *27* (12).
18. Burgert, I.; Segmehl, J.; Keplinger, T.; Schnider, T. Method for producing densified cellulosic composite material. Patent application EP17168238.8, 2017.
19. Segmehl, J. Wood and wood-derived cellulose scaffolds for the preparation of multifunctional materials. ETH Zurich, Dept. of Civil, Environmental and Geomatic Engineering, PhD thesis 24340, 2017.

20. Casdorff, K.; Keplinger, T.; Burgert, I., Nano-mechanical characterization of the wood cell wall by AFM studies: comparison between AC- and QI (TM) mode. *Plant Methods* **2017,** *13*.
21. Fengel, D.; Wegener, G., *Wood - chemistry, ultrastructure, reactions*. de Gruyter: Berlin, New-York, 1984.
22. (a) Ritchie, R. O., The conflicts between strength and toughness. *Nat. Mater.* **2011,** *10* (11), 817-822; (b) Fratzl, P.; Burgert, I.; Gupta, H. S., On the role of interface polymers for the mechanics of natural polymeric composites. *Physical Chemistry Chemical Physics* **2004,** *6* (24), 5575-5579.
23. (a) Schwager, H.; Haushahn, T.; Neinhuis, C.; Speck, T.; Masselter, T., Principles of Branching Morphology and Anatomy in Arborescent Monocotyledons and Columnar Cacti as Concept Generators for Branched Fiber-Reinforced Composites. *Advanced Engineering Materials* **2010,** *12* (12), B695-B698; (b) Müller, U.; Gindl, W.; Jeronimidis, G., Biomechanics of a branch-stem junction in softwood. *Trees-Structure and Function* **2006,** *20* (5), 643-648.
24. (a) Usov, I.; Nystrom, G.; Adamcik, J.; Handschin, S.; Schutz, C.; Fall, A.; Bergstrom, L.; Mezzenga, R., Understanding nanocellulose chirality and structure-properties relationship at the single fibril level. *Nature Communications* **2015,** *6*; (b) Salmen, L.; Burgert, I., Cell Wall Features with Regard to Mechanical Performance. A Review COST Action E35 2004-2008: Wood Machining - Micromechanics and Fracture. *Holzforschung* **2009,** *63* (2), 121-129.
25. (a) Wang, X. Q.; Keplinger, T.; Gierlinger, N.; Burgert, I., Plant material features responsible for bamboo's excellent mechanical performance: a comparison of tensile properties of bamboo and spruce at the tissue, fibre and cell wall levels. *Annals of Botany* **2014,** *114* (8), 1627-1635; (b) Bos, H. L.; Van den Oever, M. J. A.; Peters, O., Tensile and compressive properties of flax fibres for natural fibre reinforced composites. *Journal of Materials Science* **2002,** *37* (8), 1683-1692.
26. (a) Shams, I.; Yano, H.; Endou, K., Compressive deformation of wood impregnated with low molecular weight phenol formaldehyde (PF) resin I: effects of pressing pressure and pressure holding. *Journal of Wood Science* **2004,** *50* (4), 337-342; (b) Hebel, D. E.; Javadian, A.; Helsel, F.; Schlesier, K.; Griebel, D.; Wielopolski, M., Process-controlled optimization of the tensile strength of bamboo fiber composites for structural applications. *Compos. Pt. B-Eng.* **2014,** *67*, 125-131.
27. (a) Bledzki, A. K.; Gassan, J., Composites reinforced with cellulose based fibres. *Prog Polym Sci* **1999,** *24* (2), 221-274; (b) Koronis, G.; Silva, A.; Fontul, M., Green composites: A review of adequate materials for automotive applications. *Compos. Pt. B-Eng.* **2013,** *44* (1), 120-127.

TOC